



This is a repository copy of *Investigation of forced flow orientations on the burning behaviours of wooden rods using a synchronised multi-imaging system.*

White Rose Research Online URL for this paper:

<https://eprints.whiterose.ac.uk/190645/>

Version: Published Version

Article:

Lai, Y. orcid.org/0000-0002-9987-0975, Albadi, A. orcid.org/0000-0002-4564-1456, Liu, X. et al. (4 more authors) (2022) Investigation of forced flow orientations on the burning behaviours of wooden rods using a synchronised multi-imaging system. Proceedings of the Combustion Institute. ISSN 1540-7489

<https://doi.org/10.1016/j.proci.2022.07.057>

Reuse

This article is distributed under the terms of the Creative Commons Attribution-NonCommercial-NoDerivs (CC BY-NC-ND) licence. This licence only allows you to download this work and share it with others as long as you credit the authors, but you can't change the article in any way or use it commercially. More information and the full terms of the licence here: <https://creativecommons.org/licenses/>

Takedown

If you consider content in White Rose Research Online to be in breach of UK law, please notify us by emailing eprints@whiterose.ac.uk including the URL of the record and the reason for the withdrawal request.



eprints@whiterose.ac.uk
<https://eprints.whiterose.ac.uk/>



Investigation of forced flow orientations on the burning behaviours of wooden rods using a synchronised multi-imaging system

Yufeng Lai^{a,*}, Ahmed Albadi^b, Xuanqi Liu^b, Matthew Davies^a,
Matthew Hobbs^a, Jon Willmott^a, Yang Zhang^{b,*}

^a Department of Electronic and Electrical Engineering, The University of Sheffield, Sheffield, United Kingdom

^b Department of Mechanical Engineering, The University of Sheffield, Sheffield, United Kingdom

Received 4 January 2022; accepted 7 July 2022

Available online xxx

Abstract

The burning behaviour of a wooden rod under various forced flow conditions was investigated by employing a synchronised multi-imaging system integrating visible wavelength, short-wavelength infrared (SWIR), and Schlieren techniques. The wood samples were fixed horizontally and at an inclined angle to study the effect of the surface orientation under forced flow. A small-scale wind tunnel was developed to supply three types of forced flow: concurrent, opposed and cross flow. Each imaging technique helps to gain different physical insights of different aspects of the phenomenon. The combined data provides a comprehensive understanding of the flow effect on fire propagation. It was found that the forced flow strongly influences the often-invisible hot gas flow surrounding the burning rod. The heat feedback from the attached hot flow layer helped to maintain the surface temperature, which further influenced the burning behaviour. The mechanisms that the various flow orientation caused, affected the heated gas differently. Additionally, a method was proposed to monitor the burning process, which used thermal imaging to quantitatively calculate the area of pyrolysis zone on the surface. With the visualisation of the Schlieren images at the critical timings, it was found the thick hot gas flow underneath the wooden rod was a crucial factor that determined the intensity of burning, which may provide important guidance on effective wooden beam fire suppression and control.

© 2022 The Author(s). Published by Elsevier Inc. on behalf of The Combustion Institute.

This is an open access article under the CC BY-NC-ND license

(<http://creativecommons.org/licenses/by-nc-nd/4.0/>)

Keywords: Wood combustion; Forced flow; Burning behaviour; Convection; Fire spread,

1. Introduction

Small-scale cellulosic fuels have been widely used to represent the burning behaviours of fire disasters, for example, within forests or the structure

* Corresponding authors.

E-mail addresses: y.lai@sheffield.ac.uk (Y. Lai),
yz100@sheffield.ac.uk (Y. Zhang).

<https://doi.org/10.1016/j.proci.2022.07.057>

1540-7489 © 2022 The Author(s). Published by Elsevier Inc. on behalf of The Combustion Institute. This is an open access article under the CC BY-NC-ND license (<http://creativecommons.org/licenses/by-nc-nd/4.0/>)

of wooden buildings during their initiation stage of fire [1,2]; large-scale fires are typically comprised of many individual cellulosic fuels. Over the past few decades, the burning behaviour of single elements in still air, which are solely buoyancy driven, has been extensively studied and achieved remarkable progress [3,4]. The burning behaviours can be significantly changed when forced air flow is involved, since the ways of heat and mass transfer are driven by both the buoyancy and forced flow.

Concurrent flame spread, where flames spread in the same direction as the forced flow, was considered as the most rapid and hazardous [5]. Previous research has found that both the burning rate and spread rate increase with larger speeds of forced flow, until extinguishment starts [6,7]. Increased flame temperature, due to the well-mixed fuel and oxygen, was found in the research of Lai et al. [8] and Singh & Gollner [9].

With regard to forced flow opposing the flame spread direction, the flame spread rate has been investigated under microgravity conditions; the gas flow velocity characteristic is smaller than the buoyancy velocity [10,11].

In terms of the burning behaviour under cross-flow, researchers have done the comprehensive studies under stationary experiments, but very little investigation has been done for the fire propagation. Woods et al. [12] found the burning rate showed a non-monotonic response with cross flow. McAllister et al. [13] found the non-monotonic change of burning rate with increasing wind speed varied by using the different design of wooden cribs. Various techniques have been used to obtain the flame temperature distributions under cross wind [14,15].

According to the research of Wolff et al. [16] and Cristina et al. [17], convection was considered as the dominant source of heat transfer in the study of the small-scale fuel and forced flow. With regard to fire spread under still air conditions, it has been demonstrated that convective heat transfer from underneath the fuel plays the crucial role to help sustain the burning and spread of the fire [1,2,18].

Therefore, it is important to reveal how forced wind changes the flow field surrounding the burning fuel and further influences the burning behaviour. According to the literatures, several topics have yet to be studied: 1. Wind direction is considered an important factor which influences burning behaviour. However, there are no publications systematically comparing different wind directions with the same fuel. 2. Although flame behaviour has been widely studied under forced flow, there are few studies focused on the invisible hot gas flow surrounding the burning fuel. Convective heat transfer is considered an important factor which influences fire spread for small-scale fires; it is of great importance for the study of forced flow on the heat flow field. 3. The temperature of the fuel which relates

to the thermal pyrolysis has not been quantitatively analysed under forced flow conditions. In addition, the effect of the forced air flow on the fuel temperature requires further investigation.

This paper aims to reveal the effects of various wind conditions on the fire spread and burning behaviours on a single cylinder-shape wooden rod by combining different imaging techniques. The visible imaging visualises the burning behaviour of the fuel and enables qualitative measurements. The wooden surface temperature can be measured using a thermal imaging technique and used to analyse the pyrolysis zone of the fuel surface. The Schlieren imaging is used to visualise the heated flow, surrounding the burning wood, and used to analyse the convective heat transfer. With the help of the multi-imaging system, the effects of hot flow on the surface temperature and further on the burning behaviours and fire spread are presented for the first time.

2. Methodology

2.1. Experimental setup

Natural oak wood was used as the test samples. This was shaped into cylinders measuring 9.5 mm in diameter and 400 mm in length. All samples were pre-dried for 24 hours at 100 °C to keep the moisture level consistent. The apparent density was measured after pre-drying, the mean density of all the tested samples is 0.885 g/cm³ with the standard deviation 0.066 g/cm³. The samples were fixed by an adjustable holder at two orientations: 0-degree and 30-degrees. The 30-degrees was used to represent the inclined fuel surface, since it slightly beyond the critical angle [3], which dramatically enhances the fire spread.

An optimised small-scale wind tunnel with 16 cm outlet was used for the supply of forced air. The distance between the rod end and the wind tunnel was 5 cm considering the feasibility of the image systems. Five wind speeds were applied in this work: the wind speed at the location of the rod end was measured and averaged over 20 tests. The chosen speeds were: 0.47 m/s, 0.53 m/s, 0.65 m/s, 0.72 m/s and 0.87 m/s. The distribution of the wind speed was measured at the centre line of the vertical profile of the rod end, shown in Fig. 1(b). In this study, three horizontal directions of wind were used, they were: concurrent-flow, indicating the wind was parallel to or along an angle to the fire spread direction; opposed-flow, where the wind opposed or at an angle opposing the direction of fire spread; cross-flow, where the wind direction was vertical to the wooden surface, shown in Fig. 1(i) (ii) and (iii).

A premixed methane-air jet flame was used to ignite the wood samples. The burner nozzle was 5 mm in diameter, the height of visible flame was

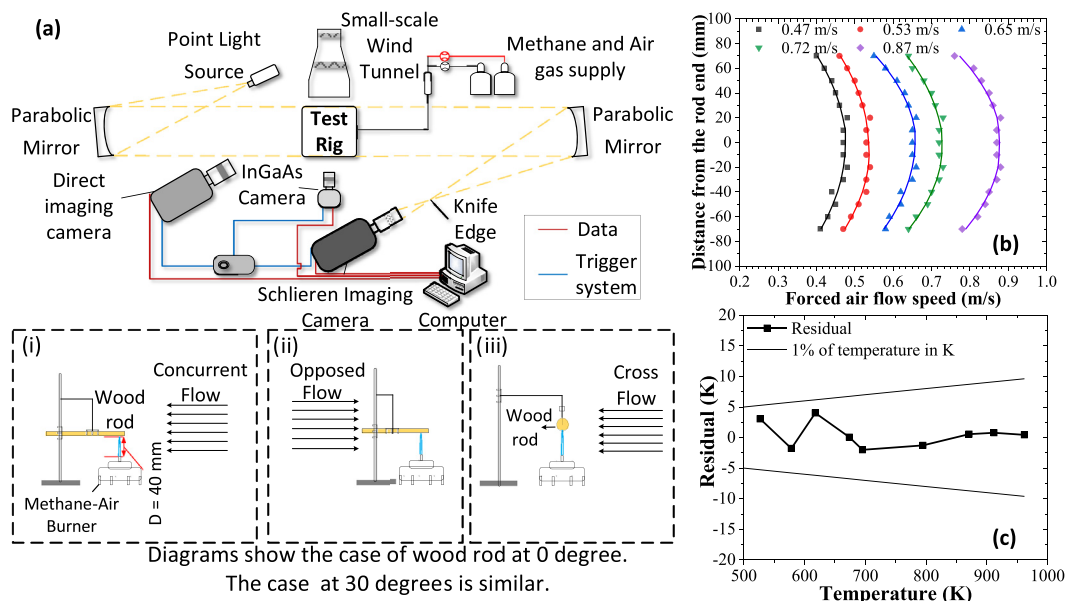


Fig. 1. Demonstration of the experimental setup (a) with various test rigs: concurrent flow (i), opposed flow (ii) and cross flow (iii). The uncertainty within the experiment: the forced air speed distributions along the centre line of the wind tunnel (b) and measured temperature residuals by the InGaAs thermal camera within the testing range ($250^{\circ}\text{C} - 700^{\circ}\text{C}$) (c).

measured as $59\text{ mm} \pm 3\text{ mm}$. Once a sample was ignited for 20 s, the burner was turned off and the wind tunnel switched on concurrently.

2.2. Imaging system

The imaging system used in the work is shown in Fig. 1(a). Three cameras were connected to a trigger system to provide a synchronised image acquisition. A high-speed colour camera was used to image the burning process directly. A short-wavelength infrared InGaAs camera was used to measure the wooden surface temperature with a cut-on filter to restrict its spectral sensitivity to $1490\text{--}1500\text{ nm}$. Finally, a monochromatic high-speed camera was used to provide a Z-type Schlieren imaging system to visualise the hot flow field around the burning rods.

2.3. Burning behaviour measurement

The visual images were used to determine the overall burning behaviour results: the burning lifetime and maximum charring distance. Each wind condition was repeated 6 times to minimise the effect of nonuniformity in the natural wood. The results present the averaged value from the repeated trials, and the standard deviation was used to present the uncertainty as error bars.

The burning lifetime was determined by the period from the start of self-sustained burning (when the ignition source was removed) to the extinguishment (no visible flame in the image). The fire

could spread throughout the whole rod with an applied concurrent flow speed of 0.47 m/s . Therefore, the burning lifetime was measured until the flame reached the top end of the rod. The burning lifetime would be able to show the extent of the self-sustained burning.

The maximum charring distance was measured as the length the char propagated from the start of self-sustained burning to the extinguishment (or throughout the whole rod). The results were normalised to show the percentage comparing the whole rod length. The charring distance was used to represent the ability of the fire spread. The overall burning behaviour could be investigated when the charring distance was combined with the burning lifetime.

2.4. Temperature measurement

The InGaAs camera was used to measure the wood surface temperature. The temperature for rapid thermal pyrolysis of wood is widely considered to be 300°C [19]. Therefore, the spectral sensitivity was restricted in the range of $1490\text{--}1500\text{ nm}$ to match the temperature range.

The calibration is based on Planck's Law, with a black body furnace (emissivity ~ 0.99) used as a standard temperature source for the calibration between 250 to 700°C , at increments of 50°C . 100 images were captured and averaged to obtain the camera's signal value at each temperature. The dark noise was determined by averaging 100 images with lens covered. A value of 0.95 was used

as the emissivity of the burning wood. This value was previously determined for the emissivity of the oak wood and the coke [20].

The main sources of uncertainty within the temperature measurements are believed to be caused by the estimation of the emissivity, and the noise of the imaging system. It can be determined by comparing the difference between the actual temperature of the furnace and the measured temperature. The maximum residual across the whole temperature range was under 1% in Kelvin, shown in Fig. 1(c). The emissivity of wood surface can vary while burning, which would cause uncertainty of temperature measurements. However, the maximum residual of temperature reading within ± 0.05 estimated emissivity value was calculated as 0.41%, which was negligible.

The measured surface temperature was presented as a colour map for visualisation. The flame emission would apply additional energy to the camera sensor which will slightly increase the temperature reading. In order to eliminate this influence, 5% of the integration intensity of the flame, which is the estimated reflecting energy of the wooden surface, has been subtracted from the wooden surface. Besides, the image of the wooden surface was cropped and the pixels with a temperature above 300 °C were averaged to show the temperature intensity at $t = 20$ s. This showed the temperature of the areas under rapid thermal pyrolysis. In addition, the size of these areas was calculated by measurement of pixel size to represent the area under the rapid pyrolysis.

3. Results and discussion

3.1. Overall burning behavior

The burning behaviour was investigated from two aspects: burning lifetime, which represents the time-wise self-sustained burning, and the maximum charring distance, which indicates the space-wise fire spread as shown in Fig. 2. All the results were measured from the visible-wavelength images.

It can be observed from Fig. 2 that the burning on the 30-degree rod was generally stronger than the case of 0-degree rod, both temporally and spatially. The studies under still air conditions [18] indicated that the 30-degree inclination significantly enhanced the charring distance, reported as 60% (30-degree) compared to 7% (0-degree). It is also observed that the ability of fire spread was significantly enhanced when the concurrent flow speed was lower than 0.72 m/s (0-degree) and 0.53 m/s (30-degree), comparing with the still air [18]. Fire spread under concurrent flow is similar to those under slope [5]. Incoming winds compete with buoyant forces which help the flames attach to the fuel surface; the 30-degree inclination further enhances this effect [8], resulting in the longest charring dis-

tance occurred under concurrent flow. The difference in the burning intensity between the two angles was most distinct under concurrent flow.

Opposed flow strongly obstructed the fire spread and it has the shortest charring distance, as shown in Fig. 2. However, the lifetime under opposed flow remained high at 0-degree, even higher than those under concurrent flow, indicating that the opposed flow helped to sustain the burning under these circumstances. Further evidence was found that the difference of burning lifetime between two rod angles was insignificant under opposed flow. This is because of a smaller wind component at the direction of fire spread when the rod was fixed at 30-degree. Another consideration is the boundary layer thickness which is different between the concurrent flow and the opposed flow. The concurrent flow would have more cooling effect on the ignition point because the boundary layer thickness increases along the rod. This could contribute to the longer burning lifetime under opposed flow and reflect the common scenarios in a real fire: one-end ignited burning.

With regards to the cross flow, the wind direction did not impact upon the direction of fire spread. Therefore, the burning intensity difference between the two angles was smaller than concurrent flow. It should be noted that the slope surface impacted positive effect on the fire spread, shown as 15% fire spread under inclination compared with 5% at horizontal.

The results showed generally how the various forced flow orientations affected the burning behaviours of the wooden rods. Consider that the flow field was strongly influenced by the forced flow, more physical insights will be shown in the next Section by visualisation.

3.2. Visualisation

Fig. 3 shows the Schlieren and thermal images at $t = 20$ s under various experimental conditions. It should be highlighted that the surface temperature of the fuel was strongly related to the surrounding hot gas flow, which was comprised of the burned gas from combustion and the combustible gases generated from the pyrolysis. Although it was widely considered that the heat flux required for the fire spread was mainly contributed by the flame feedback from the top [9,21], Fig. 3 shows the heat transfer was dominated by the convection which not only came from the top side of the fuel but also underneath the rod. When there was thick hot gas flow attached, the surface temperature remained at a high value (beyond 500 °C). In addition, the rod that had a thick hot gas layer underneath always had a longer lifetime and high intensity of burning. For example, the 0-degree rod under 0.47 m/s concurrent flow and under the high speed of opposed flow. The hot gas flow beneath the burning wood has been shown to be a crucial factor for the single

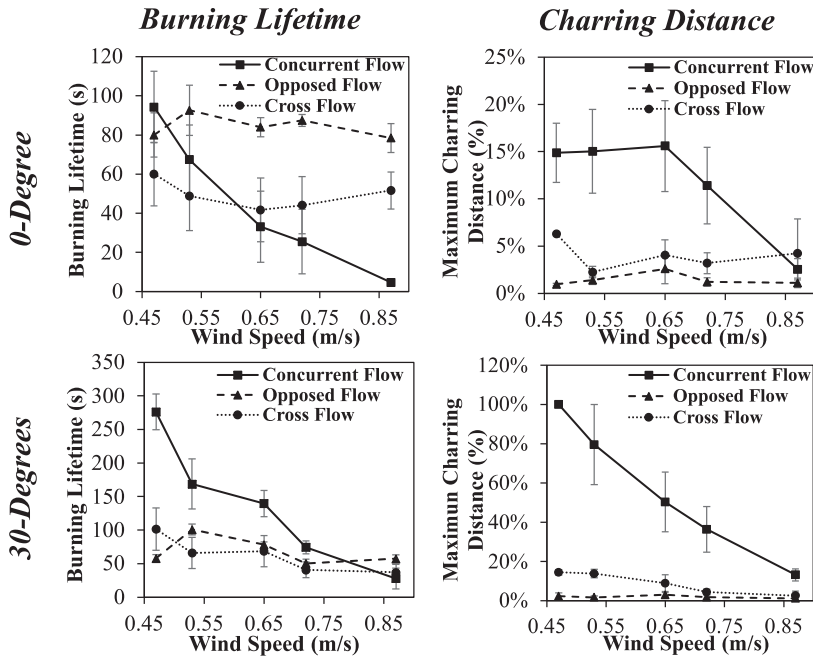


Fig. 2. Burning behaviours of rod at 0-degree (first row) and 30-degrees (second row) under various wind conditions, presented from time-wise: burning lifetime (first column) and space-wise: maximum charring distance (second column).

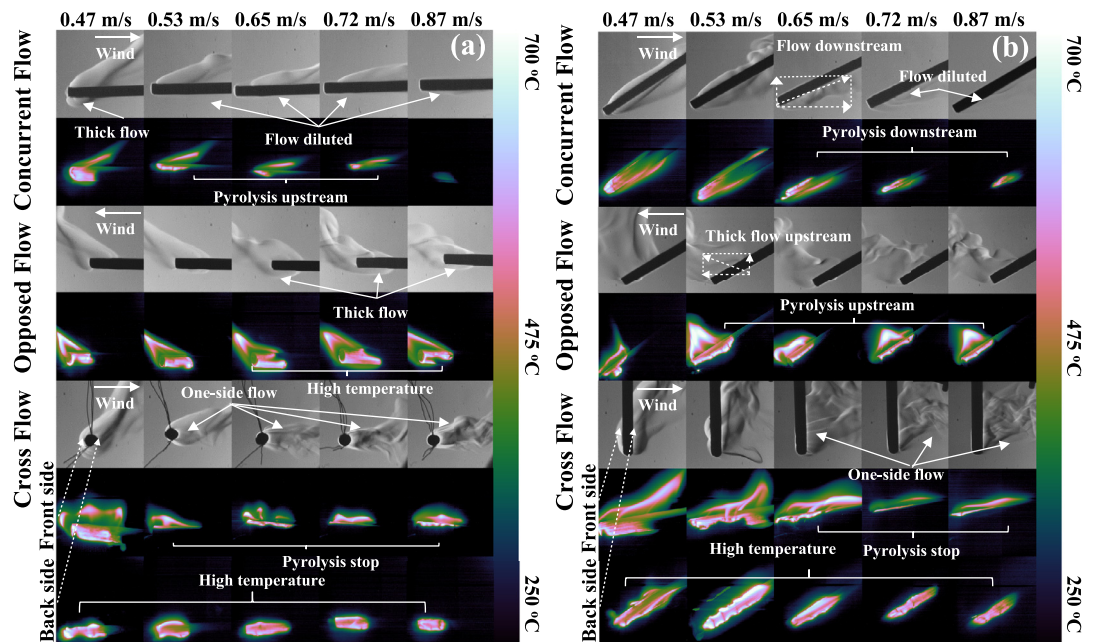


Fig. 3. Schlieren and thermal images under different wind conditions at $t = 20$ s. ($t = 6$ s for 0-degree concurrent flow 0.87 m/s). (a): 0-degree, (b): 30-degrees. For cross flow: front side indicates surface facing the wind while back side is behind the flow.

element fuel combustion [1,2,18] under still air. The mechanism by which this influences the process is the contribution to the effective heat transfer into the deep surface by the force of buoyancy [8].

Therefore, the hot gas flow changed by the forced flow determined the convective heat transfer to the virgin wood, which further affected the following burning behaviour. Specifically, the concurrent flow competed with the buoyancy and led the flame and the hot gas to attach into the fuel surface. This helped the heat transfer to the unburned wood, resulting in a longer charring distance. The impact would be stronger in the 30-degree case, due to the role inclination plays similarly in aiding the flow to adhere to the fuel surface, resulting in more effective burning and propagation in the 30-degree cases. However, the high speed of forced flow would dilute the flammable gases and increase the heat loss to the cold air, presented as the disappearance of the flow underneath the 0-degree rod. When the wind speed was higher than 0.53 m/s, the pyrolysis zone moved upside. Regarding the 30-degree rod, the density of underneath flow was higher since the gas-phase combustion occurred in this region. Consequently, the thick underneath hot gas was present when the speed was 0.72 m/s. On the other hand, the high speed of forced flow prevented the heat transferring upward effectively. There was no hot gas on the top side, therefore, the pyrolysis moved downside.

The opposed flow impacted the flame on the top and increased the angle between the flame and the unburned wood. This phenomenon had also been reported by other researchers [11]. The additional observation in this work is that opposed flow also impacted on the underneath hot gas flow which can only be seen in the Schlieren image. The underneath flow started to appear with the 0-degree rod when the wind speed increased to 0.53 m/s, and was greatest when the speed was 0.65 m/s. It can, therefore, be considered as the point at which heat feedback from the hot gas was greatest. It was shown that the hot gas flow helped the surface remain at a high temperature, and the area under pyrolysis was large, by comparing the thermal imaging at the same time. Therefore, the opposed flow helped the 0-degree rods sustain longer than other flow directions (see Fig. 2). On the other hand, the opposed flow prevented the flow from moving to the unburned surface, leading to a short charring distance. The opposed flow influenced the hot gas flow in a different way when the rod was inclined. The underneath flow was pushed into the top surface as shown in Fig. 3. The underneath flow appeared only at the wind speed 0.47 m/s and the heated length in the bottom surface was shorter than on the top side. Consequently, the burning lifetime stayed short as shown in Fig. 2.

The crossflow did not directly impact on the direction of fire spread, however, it influenced the area under convective heating [22]. Both orienta-

tions had the thick hot gas flow layer surrounding the rods under the cross flow speed 0.47 m/s. Therefore, more wooden fuel was heated and took part in the pyrolysis, which can be found in the thermal images of both sides. This phenomenon was reflected in the burning lifetime that the rods under 0.47 m/s could sustain the longest. When the wind speed increased, the hot gas flow layer on the front side disappeared. Resulting in the surface temperature on this side becoming significantly decreased. A similar phenomenon has been visualised by direct imaging in [17] and the visible flame is only concentrated on the back side of the rod, reducing the fuel pyrolysis. The 30-degree rods exhibited a similar phenomenon. However, one difference was that the sloped surface supplied a positive effect on the flame propagation and both the flame and flow would tend to attach to the unburned surface. Therefore, the fire under low-speed crossflow could spread a finite distance, around 15% according to Fig. 2. When the wind speed was larger than 0.65 m/s, the cross flow dominated the effect of the hot gas flow direction and made the fire rarely propagating.

3.3. Surface temperature

The forced flow directly influenced the temperature and further affected the burning behaviours. It has been reported by Lai et al. [8] that the flame temperature slightly increased when the concurrent flow speed was lower than 0.49 m/s and dropped dramatically at higher speed when similar fuel was used. Singh & Gollner [9] measured the diffusion flame temperature profile and found the peak temperature decreased at high flow speed. From the images in Fig. 3, it is observed the surface temperature was not only contributed to by the radiation from the soot but also the convection from the surrounding hot gas flow. The heat feedback from the flame and hot gas flow both impacted on the surface temperature. The high-resolution thermal camera allowed to see the fuel surface temperature distributions. The pixels whose temperature was above 300 °C were averaged to show the average temperature intensity under various flow conditions because it is widely agreed that the rapid thermal pyrolysis starts around 300 °C [19]. The front side had already cooled down at $t = 20$ s under cross flow, therefore, the results of cross flow only presented the surface of the back side. The area of these zones was calibrated and calculated to indicate the size of the pyrolysis zone.

Fig. 4 presents the mean temperature and area of the rapid thermal pyrolysis zones ($T > 300$ °C). The results present the averaged value from the repeated trials, and the standard deviation was used to present the uncertainty as error bars. Generally, the mean temperature decreased with the higher speed of flow. This phenomenon can be explained by several factors: 1. The increased heat loss from

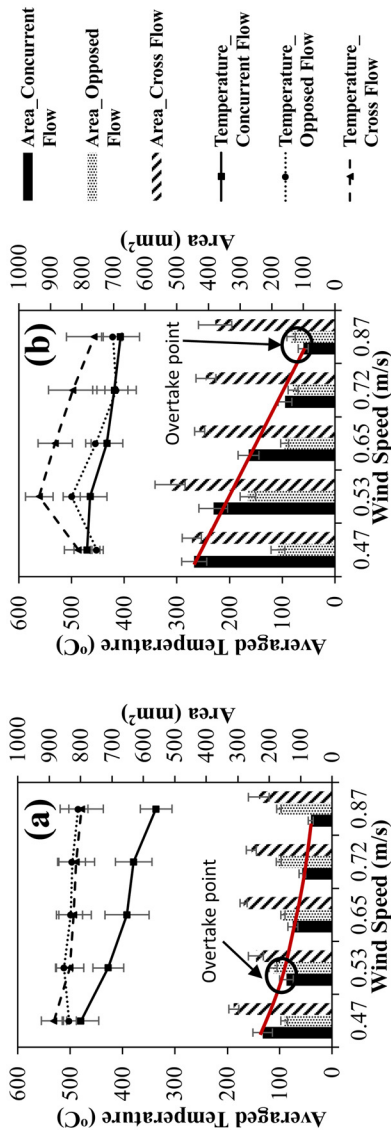


Fig. 4. Average surface temperature and area of the pyrolysis zone ($T \geq 300$ °C) under different wind conditions at $t = 20$ s ($\tau = 6$ s for 0-degree concurrent flow 0.87 m/s). (a): 0-degree, (b): 30-degrees. The error bars indicate the standard deviation of repeated trials.

the surface to the cold air because the higher speed of flow increases the convective heat transfer coefficient; 2. Heat feedback from the flame decreased due to the flame temperature drop at higher wind speed [8,9]; 3. The hot gas flow layer generally became thinner with higher wind speed according to Fig. 3. More specifically, the mean temperature under concurrent flow had significantly decreased as wind speed increases. Reversely, the opposed and cross flows had an indistinct temperature drop. This interesting phenomenon further indicates that convective feedback was dominant at this scale of fire: although the opposed and cross flows pushed the flame away from the fuel surface, the surface temperature under those two wind directions remained high. The high surface temperature resulted from the thick hot gas flow attached to the wooden rod, shown in the Schlieren images under opposed flow and cross flow (back) in Fig. 3. Conversely, the concurrent flow brought the flammable gases and burned gases away and heated the virgin wood. Therefore, it diluted the underneath hot gas layer, as shown in the Schlieren images under high speed of concurrent flow in Fig. 3. The surface temperature consequently decreased. In terms of opposed flow, the high surface temperature and short spread distance enhanced the consumption of the local fuel. The burning lifetime for these cases can, therefore, be considered as the burned-out time for the limited fuel.

The histogram shows the surface area size under rapid pyrolysis. It should be highlighted that the area decreased monotonically with the higher wind speed under concurrent flow at both orientations of rod, shown as a red line in Fig. 4. Fig. 3 highlighted the phenomenon of pyrolysis upside at 0-degree and pyrolysis downside at 30-degrees which was caused by the disappearance of hot flow underneath (0-degree) or topside (30-degrees). Nevertheless, the change of location of the attached hot gases resulted in the decreased area of the pyrolysis zone.

Regarding the pyrolysis zone under opposed and cross wind, there was insignificant change with the wind speed. This indicates that the area enfolding by the hot gas layer did not change significantly. On the other hand, the fire could not spread effectively in these two directions of wind.

The pyrolysis zone decreased under high-speed concurrent flow. Fig. 4 highlighted the wind speed at which the area under opposed flow overtook concurrent flow. These were 0.53 m/s for 0-degree and 0.87 m/s for 30-degrees. These coincided with the burning lifetime in Fig. 2. A hypothesis may be posited that the less fuel feeding the pyrolysis may lead to the shorter burning lifetime.

3.4. Burning process

The burning rate has been used as the indicator for monitoring the burning process in the mass

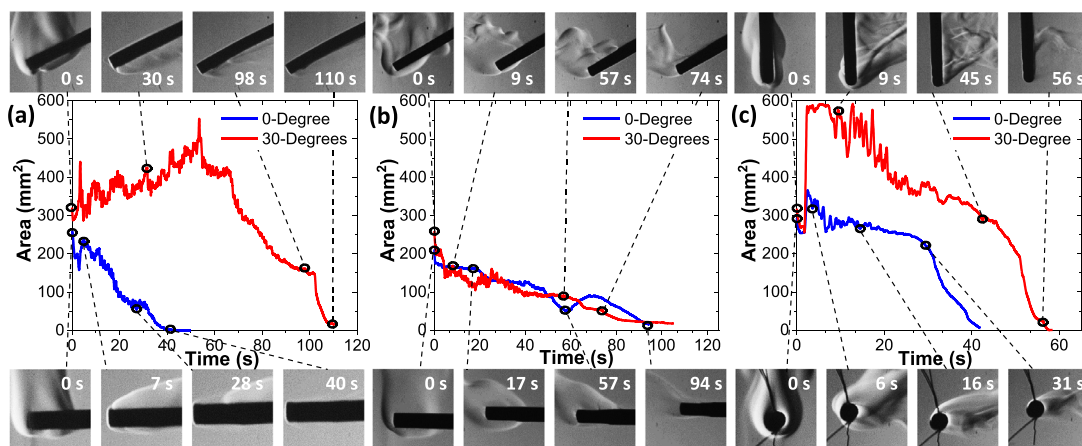


Fig. 5. The diagram of pyrolysis zone area ($T \geq 300^\circ\text{C}$) against time and presented with Schlieren images at typical timings: initiation, high-intensity burning, low-intensity burning and extinguishment under wind speed 0.65 m/s. (a): concurrent flow; (b): opposed flow; and (c): cross flow.

transfer [23]. This work proposed a new way to present the different stages of the burning process by monitoring the pyrolysis zone area. The pyrolysis zone on the surface can be determined with the use of the thermal images. The larger the area of pyrolysis indicated the more wooden surface would be affected by the rapid pyrolysis.

Fig. 5 shows the area of the pyrolysis zone against time at a speed of 0.65 m/s for different wind directions. The hot gas flow was the most significant factor that influenced the surface temperature, further affecting the burning behaviours. The Schlieren images at typical timings are used to explain the phenomenon of pyrolysis area change. It can be found that the burning process presented similar characteristics under the same flow direction of 0-degree and 30-degrees rods, but on a different scale. Specifically, the area under concurrent and cross flow on the inclined surface was larger than 0-degree and resulted in a longer life-time. The difference was more significant under the concurrent flow than the cross flow. This was because the 30-degrees inclination enhanced the upward flame propagation by increasing the preheating from the underneath surface [18]. The cross flow did not have an influence on the underneath preheating while the concurrent flow forced the flow into the bottom of the rod and enhanced the preheating from the underneath. This is shown in the Schlieren images of concurrent flow. Conversely, there was negligible difference between the burning behaviours between 0-degree and 30-degrees rods under the opposed flow. This can be explained by the decreased underneath hot gas flow caused by the opposed flow at 30-degrees. Part of the hot gas layer from underneath of rod was forced upside which was highlighted in Fig. 3. The decreased underneath hot gas counteracted the positive effect of the fire spread from the inclination. Contrar-

ily, the thicker underneath hot gas flow in the 0-degree rod was pushing back to the initial burning location.

With regards to the burning process at different timing, the four Schlieren images showed the typical timings as: the initiation, the high-intensity of burning (pyrolysis area at a high level), low-intensity of burning (pyrolysis area starts to drop sharply) and extinguishment respectively. It should be highlighted that there was thick hot gas layer underneath the rod when the high intensity of burning proceeded. When the hot gas layer has gone, the pyrolysis area declined quickly and the intensity of the burning started to weaken. Researchers had investigated that the underneath preheating played a critical role for the thick fuel burning under still air [1,2,18]. It can be concluded from Fig. 5 that the underneath flow was considered as the crucial factor determining the intensity of burning under forced wind.

For the concurrent flow, the dilution of the flammable gases and the increased heat loss by the forced air decreased the burning intensity. In addition, the concurrent wind under 0.65 m/s prevented effective heat transfer from the bottom of rod to the topside causing less fuel to be consumed by the pyrolysis resulting in the decreasing hot gas flow produced. Therefore, the fire could not be sustained, and the burning stopped. Regarding the opposed flow, this wind direction effectively prevented the fire from spreading. The fire spread required both the heat and mass transfer into the unburned fuel [24]. However, the opposed flow impeded the flammable gases and the convection from the hot gas flow transfer into the virgin wood. Once there was not enough hot flow generated by the pyrolysis and the flaming burning, the burning became weaker and then stopped. The similar effect of concurrent and opposed flow can be found

in the cross flow direction. The wood burning remained at a high intensity before $t = 20$ s. However, with the consuming of the wood fuel, the produced flammable gases decreased with time. There was not enough fuel supplied since the cross flow did not aid the spread of the fire, but increased the dilution of the gas fuel. Therefore, the hot gas flow became thinner causing the wood to stop burning.

4. Conclusions

The effects of various forced flow conditions on the burning behaviour of wooden rods were investigated visually and quantitatively using multiple imaging systems and a non-contact temperature measurement instrument. It was found that the forced flow strongly influenced the hot gas flow surrounding the burning rod and further affected the fuel surface temperature. A new method was proposed to monitor the burning process by determining the area of the pyrolysis zone on the surface. Several conclusions can be drawn from this work:

1. The inclination of the rod can have a similar effect to the concurrent flow by enhancing the attachment of the flow into the fuel.
2. The concurrent flow helped the fire spread by increasing the length of the attached hot gas flow into the virgin wooden fuel. The enhanced heat loss and the dilution of the flammable gases led the surface temperature to drop, resulting in the lower intensity of burning under high wind speeds.
3. The opposed flow prevented the fire spread by impeding the heat and mass transfer to the unburned surface. However, the surface temperature remained high at this wind condition, resulting in the high intensity of the local burning.
4. The cross flow can be considered as the combination of the dilution of the hot gas flow and the obstruction of the fire spread. The hot gas flow was forced to one side of rod reducing fuels contributing to the pyrolysis.
5. The underneath hot gas flow was found to be a crucial factor in sustaining the burning and was strongly affected by the different flow orientations. This observation is of great importance for wooden beam fire control and suppression.

Declaration of Competing Interest

The authors declare that they have no known competing financial interests or personal relationships that could have appeared to influence the work reported in this paper.

Acknowledgments

Authors would like to thank the Leverhulme International Fellowship (ID/Ref: IAF-2019-034) in getting this work initiated.

References

- [1] R. Weber, N.D. Mestre, Flame spread measurements on single ponderosa pine needles: effect of sample orientation and concurrent external flow, *Combust. Sci. Technol.* 70 (1–3) (1990) 17–32.
- [2] T. Hirano, S.E. Noreikis, T.E. Waterman, Measured velocity and temperature profiles near flames spreading over a thin combustible solid, *Combust. Flame* 23 (1) (1974) 83–96.
- [3] Y. Wu, H. Xing, G. Atkinson, Interaction of fire plume with inclined surface, *Fire Saf. J.* 35 (4) (2000) 391–403.
- [4] L. Hu, A review of physics and correlations of pool fire behaviour in wind and future challenges, *Fire Saf. J.* 91 (2017) 41–55.
- [5] M.J. Gollner, C.H. Miller, W. Tang, A.V. Singh, The effect of flow and geometry on concurrent flame spread, *Fire Saf. J.* 91 (2017) 68–78.
- [6] A.V. Singh, M.J. Gollner, Steady and transient pyrolysis of a non-charring solid fuel under forced flow, *Proc. Combust. Inst.* 36 (2) (2017) 3157–3165.
- [7] J.I. Cuevas, A. Guibaud, C. Maluk, J.L. Torero, Understanding flame extinction in timber under external heating using high-activation energy asymptotics, *Combust. Flame* 235 (2022) 111645.
- [8] Y. Lai, X. Wang, T.B. Rockett, J.R. Willmott, Y. Zhang, Investigation into wind effects on fire spread on inclined wooden rods by multi-spectrum and schlieren imaging, *Fire Saf. J.* 127 (2022) 103513.
- [9] A.V. Singh, M.J. Gollner, Local burning rates and heat flux for forced flow boundary-layer diffusion flames, *AIAA J.* 54 (2) (2016) 408–418.
- [10] F. Zhu, Z. Lu, S. Wang, Y. Yin, Microgravity diffusion flame spread over a thick solid in step-changed low-velocity opposed flows, *Combust. Flame* 205 (2019) 55–67.
- [11] S. Hossain, I.S. Wichman, F.J. Miller, S.L. Olson, Opposed flow flame spread over thermally thick solid fuels: buoyant flow suppression, stretch rate theory, and the regressive burning regime, *Combust. Flame* 219 (2020) 57–69.
- [12] J.A. Woods, B.A. Fleck, L.W. Kostiuik, Effects of transverse air flow on burning rates of rectangular methanol pool fires, *Combust. Flame* 146 (1–2) (2006) 379–390.
- [13] S. McAllister, M. Finney, The effect of wind on burning rate of wood cribs, *Fire Technol.* 52 (4) (2016) 1035–1050.
- [14] R.G. Salvagni, M.L.S. Indrusiak, F.R. Centeno, Biodiesel oil pool fire under air crossflow conditions: burning rate, flame geometric parameters and temperatures, *Int. J. Heat Mass Transf.* 149 (2020) 119164.
- [15] K. Himoto, Quantification of cross-wind effect on temperature elevation in the downwind region of fire sources, *Fire Saf. J.* 106 (2019) 114–123.
- [16] M. Wolff, G. Carrier, F. Fendell, Wind-aided fire-spread across arrays of discrete fuel elements. II. Ex-

- periment, *Combust. Sci. Technol.* 77 (4–6) (1991) 261–289.
- [17] G. Di Cristina, N.S. Skowronski, A. Simeoni, A.S. Rangwala, S.-k. Im, Flame spread behavior characterization of discrete fuel array under a forced flow, *Proc. Combust. Inst.* 38 (3) (2021) 5109–5117.
- [18] Y. Lai, X. Wang, T.B. Rockett, J.R. Willmott, H. Zhou, Y. Zhang, The effect of preheating on fire propagation on inclined wood by multi-spectrum and schlieren visualisation, *Fire Saf. J.* 118 (2020) 103223.
- [19] D. Drysdale, *An introduction to fire dynamics*, John Wiley & Sons, 2011.
- [20] M.J. DiDomizio, P. Mulherin, E.J. Weckman, Ignition of wood under time-varying radiant exposures, *Fire Saf. J.* 82 (2016) 131–144.
- [21] A.V. Singh, M.J. Gollner, A methodology for estimation of local heat fluxes in steady laminar boundary layer diffusion flames, *Combust. Flame* 162 (5) (2015) 2214–2230.
- [22] X. Ju, M.J. Gollner, Y. Wang, W. Tang, K. Zhao, X. Ren, L. Yang, Downstream radiative and convective heating from methane and propane fires with cross wind, *Combust. Flame* 204 (2019) 1–12.
- [23] L. Hu, C. Kuang, X. Zhong, F. Ren, X. Zhang, H. Ding, An experimental study on burning rate and flame tilt of optical-thin heptane pool fires in cross flows, *Proc. Combust. Inst.* 36 (2) (2017) 3089–3096.
- [24] F. Williams, Mechanisms of fire spread, in: *Symposium (International) on Combustion*, volume 16, Elsevier, 1977, pp. 1281–1294.